Liquids sensor/detector using an EBG structure

S. Jun, B. Sanz-Izquierdo, and E.A Parker

***Abstract*—This paper describes a novel procedure to detect liquids with various permittivities using an electromagnetic band gap (EBG) structure. The concept can also be used as a method to achieve antenna frequency tunability. The main sensor consists of an array of square patches on a square unit cell with a series of cuts and grooves in the dielectric material between the patches. These trenches allow for the deposition of the liquids to be detected. The variation in the dielectric characteristics of the liquids inserted produces a change in the reflected phase of the EBG. This change in phase could be detected in various ways. In this paper, a planar antenna has been placed at a short distance from the EBG structure. The changes in the phase in the surface waves produce a change in the reflection coefficient of the antenna. Butan-1-ol, propan-2-ol, ethanol and methanol have been inserted to demonstrate the tuning technique. In order to complete the experiments the reflection coefficients and the radiation patterns were measured. Good agreement has been found between simulated and measured results. The envisaged detector could be used in a laboratory or clean room where liquids may fall into the channels.**

***Index Terms*—Electromagnetic bandgap, periodic structures, liquid antenna, CPW antenna.**

I. Introduction

ELECTROMAGNETIC BAND GAP (EBG) structures have been a popular research topic in the antenna and microwave electronics community ever since they were invented more than two decades ago [1]-[3]. EBG structures consist of periodic arrays of elements that are able to resonate at a wavelength significantly larger than the size of their unit cell. The structures are normally realized by periodic dielectric and metallic elements which interact to suppress surface waves generated by incident waves in a particular frequency band. The EBG structures are incorporated with an antenna for various modern wireless communication applications, such as wireless body area networks [4], telemedicine applications [5], global positioning systems (GPS) [6], and UHF radio frequency identification (RFID) packaging [7], to improve the overall antenna performance. In addition, millimeter wave EBG structures for antennas are introduced in [8], [9].

Reconfigurable or tunable capability can be generated by a phase change of an EBG structure using a variety of techniques. In the published literature, reconfiguration is accomplished by using varactor diodes, PIN diodes or RF microelectromechanical systems (MEMS) switches. Reconfigurable operating frequency [10], [11] and polarization reconfiguration [12], [13] are possible through variation of the EBG characteristics. A combination of them is presented in [14]. Moreover, phase variations across the EBG array have even been realized by employing mechanical movement of the elements [15].

The concept of reconfigurable antennas and radio frequency (RF) devices has found applications in the area of sensors and detectors [16] - [23]. In [16], the temperature dependence of the dielectric constant of the substrate of a microstrip patch antenna is used as a sensor. There, the variations in dielectric permittivity as a function of temperature has shown to have an effect on the resonant frequency of the antenna. Similarly, a reconfigurable slot patch antenna is used to sense environmental temperature changes in [17]. In order to increase sensitivity, the structure is filled with distilled water.

Detecting liquids have been proposed using a variety of RF techniques [18] - [23]. In [18], the dielectric permittivity of various liquids is detected using a low cost chipless RFID sensor consisting of a planar substrate integrated waveguide (SIW) structure connected to radiating antennas. Metamaterial-based liquid sensors based on various detection processes are described in [19] - [23]. One of the earliest concept of metamaterial sensor can be found in [19], where it was demonstrated that the resonant frequency of a frequency selective surface (FSS) can change when using a liquid substrate. More recently, a split-ring resonator FSS array has been theoretically proposed for thin-film sensing and sensing of liquid properties in [20]. A complementary split ring resonator has also been used in combination with a microchannel to create a highly-sensitive dielectric sensor in a two-port device [21]. In [22], a disposable solution for sensing liquids using a metamaterial is fabricated using printing technologies. In related area of research, a patch with metamaterial features is proposed as a biosensing platform for adulteration detection in oil in [23].

In this paper, we present a novel sensor/detector technique, taking advantage of the different dielectric permittivities of a range of liquids, and the change that they can produce on an EBG structure. A planar EBG structure is modified to introduce trenches between square unit cell elements, cut using a high

Manuscript received June 7, 2018: revised …., and ……..…; accepted….

This work was supported by in part by the UK EPSRC High Value Manufacturing Fellowship (REF: EP/L017121/1), in part by the EPSRC grant (REF: EP/S005625/1) and in part by the Royal Academy of Engineering Industrial Secondment scheme (REF: ISS1617/48).

S. Jun, B. Sanz-Izquierdo, and E. A. Parker are with the School of Engineering and Digital Arts, University of Kent, Canterbury CT2 7NT, U.K. (e-mail: sj329@kent.ac.uk; b.sanz@kent.ac.uk ; e.a.parker@kent.ac.uk).

Color versions of one or more of the figures in this paper are available online at http://ieeexplore.ieee.org.

Digital Object Identifier

precision milling machine. The created trenches are filled with liquids of different dielectric permittivities. These change the reflection phase of the EBG structure. A modified circular slot antenna with a coplanar waveguide (CPW) feed line is mounted above the center of the trenched array. By controlling the dielectric permittivities in the trenches, the resonant frequency of the antenna can be tuned.

The paper is organized as follows. In Section II, the details of the geometry of the unit cell element with trenches and its characteristics are described. After that, a wideband CPW antenna is designed and optimized on a planar EBG array. Section III studies the frequency tuning ability of the trenched EBG through investigations using a range of liquid permittivities. Finally, the paper concludes with the discussion in Section IV. All designs of the antennas investigated have been optimized using the finite integration technique (FIT) techniques included in CST Microwave Studio™.

II. EBG SENSOR/DETECTOR

A. *Unit cell design with trenches*

Fig. 1 shows the geometry of the unit cell element with their trenches. A square patch is used as the unit cell element which is on the center of the substrate. The phase reflection response of the unit cell element geometry is typically determined by the thickness and relative dielectric permittivity of the substrate. It is designed on an RT/duroid 5870 substrate with dielectric constant of $\varepsilon_r = 2.33$, loss tangent of $tan\,\delta = 0.0005$ and thickness of 3.175 mm. A conducting ground plane is on the other side of the substrate. Trenches are introduced by removing the substrate partially surrounding the square patch as shown in Fig. 1(a). They interrupt surface wave propagation, thereby changing the reflection phase characteristics of the planar unit cell element [24]. Moreover, the depth of the trenches can modify the various surface-wave modes without changing the overall square patch size. By adjusting the patch size, the unit cell element on the planar substrate can be set to give a resonant frequency of 2.45 GHz (see below). The gap distance between the conducting square patch sides and the edge of the unit cell element is 2 mm in that case. Table I shows the main design parameters, including those of the unit cell, ie. the original planar EBG structure. In all cases, the conducting patch on the front (Fig. 1) is 33.45 mm square and the ground plane on the back is 37.45 mm square.

The computational model for reflection phase characterization of the unit cell element with trenches, simulated using the periodic boundary condition (PBC) option in CST, is shown in Fig. 1(b). Applying this condition (PBC) on the side walls and waveguide port at the top provides an incident plane wave, enabling extraction of the dispersion diagram of the unit cell element in an infinite EBG array structure. A periodic structure consisting of square patches can be described by an inductance-capacitor (LC) circuit with distributed capacitors and inductors. The inductance (L) is determined by the distance between the square patches and the ground plane and the capacitor (C) is characterized from the gap between the square patches.

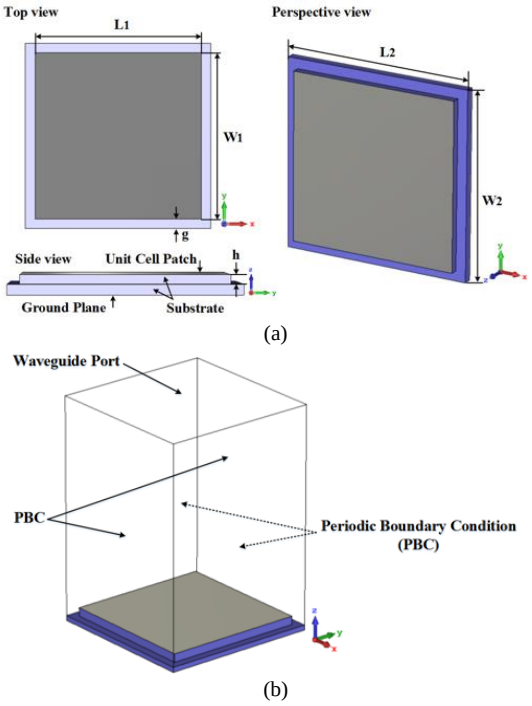

Fig. 1. (a) Geometry and (b) Infinite model of the unit cell element with trenches.

TABLE I
DIMENSIONS OF UNIT CELL GEOMETRY [mm]

L1	*W1*	*L2*	*W2*	*g*
33.4	33.4	37.4	37.4	2

The surface impedance and resonant frequency of the periodic structure are calculated respectively as follows [1]:

$$Z = \frac{j\omega L}{1-\omega^2 LC} \tag{1}$$

$$\omega_0 = \frac{1}{\sqrt{LC}} \tag{2}$$

The resonant frequency can therefore be controlled by the gap between patches and the thickness of the substrate. The bandwidth of the periodic structure is also given by

$$BW = \frac{1}{\eta_0}\sqrt{\frac{L}{C}} \tag{3}$$

where η_0 is the free space impedance. The operational resonant frequency and the bandwidth provided by the unit cell element is normally taken as the frequency of zero degree reflection phase, and the frequency band corresponding to the phase range of -90° to +90°. Over this range, the phase does not critically influence the reflected signal power [3]. Therefore, the operating frequency band of the EBG can be determined by the design of the square unit cell element.

Fig. 2 shows the computed reflection phase response of the unit cell element, illustrating the effects of partially removing the substrate, ie. varying the depth of the trenches. The resonant

frequency (zero degree phase) in Fig. 2 occurs at 2.45 GHz, 2.50 GHz, 2.53 GHz, 2.56 GHz and 2.57 GHz respectively. The resonant frequency increases, but the bandwidth is not changed when the depth is varied from 0 to 2 mm. This might be expected, since the effective dielectric permittivity of the substrate is reduced by the partial removal of the substrate from the periphery. Fig. 3(a) shows the computed sensitivity of the unit cell element with the trenches filled with various liquids, as indicated by the resonance frequency and wavelength in the reflection phase response. The loss tangent was set to 0 when the dielectric constant was changed from 1 to 15. In all cases, the depth of the trenches was 1 mm. The change in permittivity led to a change in resonant frequency that fits to a quadratic equation, although as a sensor, it is best to use a linear variation between the x and y variables. The change in operating wavelength here can meet this requirement approximately. It can be expressed by a linear equation of the form:

$$y = 0.0027x + 0.1162 \quad (4)$$

where x is the dielectric constant and y is the wavelength in meters. The R-squared obtained is about 99.7%. Fig. 3(b) shows the effect of varying the loss tangent from 0 to 9 when the dielectric constant is set to 2. The change in loss tangent had no appreciable effect on the resonant frequency.

B. Antenna on planar EBG substrate: preliminary trials

Before applying the unit cell element with trenches (Fig. 1) to periodic array structures, a CPW antenna on a planar EBG structure is designed and tested in this section. Fig. 4 shows the geometrical configuration of this antenna. The antenna is composed of a CPW feed line and a modified circular radiator with slots. This is a well known design able to produce an omnidirectional radiation pattern over a wide bandwidth [25]. The slots have been added to the radiating structure solely for the purpose of fine tuning when placed on the EBG structure. The substrate employed was an RT/duroid 5880 with relative permittivity of $\varepsilon_r = 2.20$, loss tangent of $tan\ \delta = 0.0004$ and thickness 1.575 mm. The overall dimension of the antenna was 60 mm x 60 mm. The antenna was placed on the center of the planar EBG structure as shown in Fig. 4 (c). The EBG consisted of a 3x3 array of unit cell elements. This was found to be the smallest array able to produce the required resonant frequency and antenna impedance match effectively (S_{11} < -10dB). The dimension of the square patch employed in the unit cell was 33.4 mm x 33.4 mm, as in Section II A and in Fig. 2. The overall dimension was 111 mm x 111 mm. The separation between the antenna and the EBG structure was set to 5 mm, the optimum for the Bluetooth frequency of 2.45 GHz.

The fabricated structure is shown in Fig. 5. A 50 ohm SMA connector is attached to the feed line. To fix the distance between the antenna and the EBG structure, in initial trials rectangular non-conductive polystyrene foams ($\varepsilon_r \approx 1$) with thickness of 5 mm were attached behind the corners of the antenna and topside of the EBG structure, using double sided adhesive tapes. Fig. 6 shows a comparison of the reflection coefficient of the antenna, with and without the EBG structure.

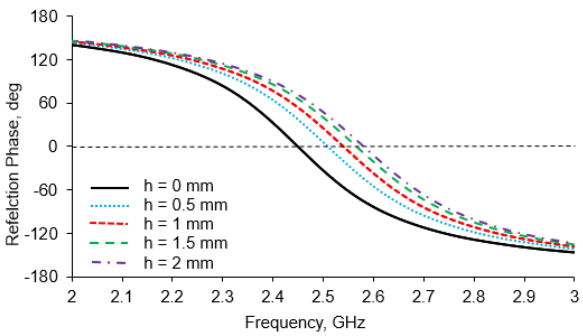

Fig. 2. Unit cell with trenches: calculated dependence of reflection phase on trench depth (h).

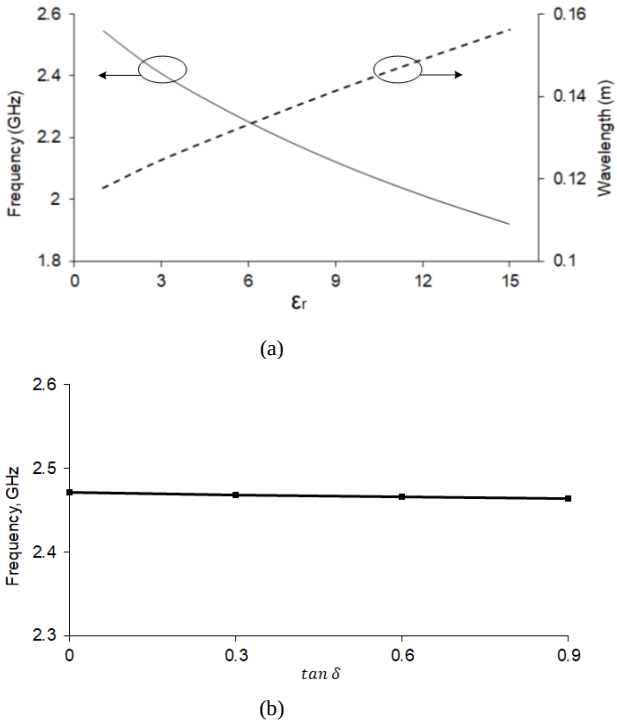

Fig. 3. Sensitivity of the resonance frequency to (a) dielectric constant (ε_r) (b) loss tangent ($tan\ \delta$) of liquids in the trenches.

An Anritsu 37397C vector network analyzer was used for the reflection coefficient measurement. The measured frequency range of the antenna alone is from 1.9 GHz to 3.3 GHz, the -10dB points of the reflection coefficient response. It has a *broad* bandwidth of about 52%. On the other hand, the antenna on the planar EBG structure has a measured -10dB bandwidth of just 14%, from 2.3 GHz to 2.7 GHz. The null is deep at 2.45 GHz: -36.5 dB. As the results show, the EBG structure provides a narrow bandwidth and deeper resonance compared with the antenna alone. Fig. 7 presents the measured normalized radiation patterns. They are also compared with the radiation pattern of the antenna alone. They were measured at 2.45 GHz in the *xz* and *yz* planes in an anechoic chamber. As shown in the results, the antenna alone has omnidirectional radiation patterns in all planes. However, the radiation pattern of the antenna on the planar EBG structure is more directional. The front-to-back ratio of the radiation pattern is improved by about 20 dB.

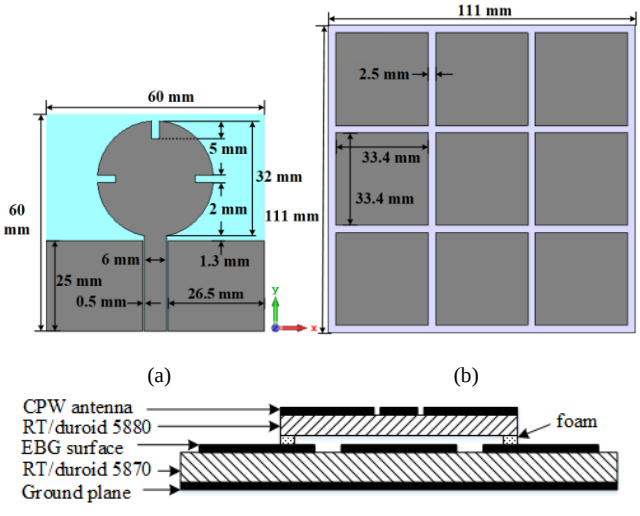

Fig. 4. (a) Top view of CPW antenna and (b) EBG structure (c) Side view of CPW antenna on planar EBG structure.

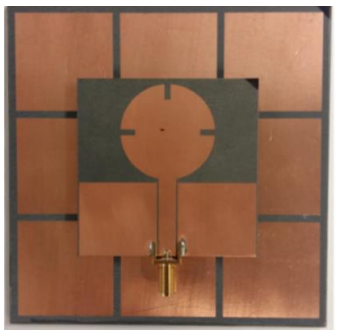

Fig. 5. Photograph of the fabricated CPW antenna on planar EBG structure.

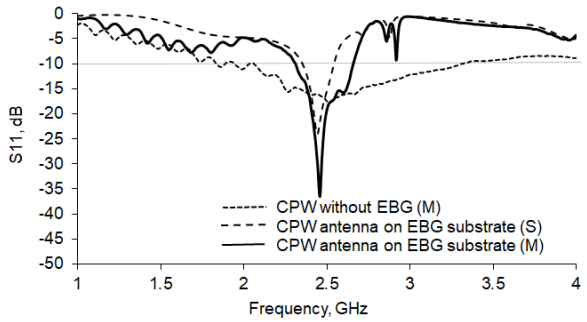

Fig. 6. Reflection coefficient (S_{11}) of the CPW antenna on planar EBG structure (S: Simulation, M: Measurement).

The gain of the antenna combined with the EBG structure is enhanced by 6.8 dB as compared with that of the antenna alone.

III. EBG SENSOR/DETECTOR ANTENNA

A. *EBG structure design with trenches*

Fig. 8 presents the geometry of the antenna on an EBG structure with trenches. The concept of a unit cell with trenches (Fig. 1) is extended to a periodic EBG structure. The overall dimensions of the new array are 111 mm x 111 mm, consisting of 9 unit cell elements each of size 33.4 mm x 33.4 mm, the same dimensions as the previous trial array (Fig. 4).

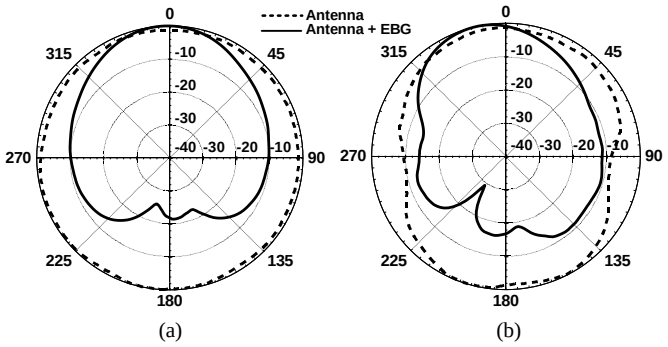

Fig. 7. Measured radiation pattern of the CPW antenna in free space and on planar EBG structure at 2.45 GHz (a) *xz* plane (b) *yz* plane.

The difference between them is the presence of the trenches. As mentioned in Section II, these are made by removing material from the substrate. The width and depth of the trenches are referred to as *w* and *h*. As shown in Fig. 2, the unit cell element with 1 mm trench depth has zero phase reflection response at 2.54 GHz. The same CPW antenna (Fig. 4) is placed over the trenched array at height of 5 mm.

Fig. 9 shows the computed reflection coefficients of the antenna for different trench depths (*h*) ranging from zero to 2 mm in 0.5 mm steps. The width (*w*) of the trenches is fixed at 2.5 mm for the investigation. The frequency increases when the depth of the trenches increases. The null in the reflection coefficient occurs at 2.45 GHz, 2.47 GHz, 2.54 GHz, 2.57 GHz and 2.58 GHz respectively. The variations in resonant frequencies are very close to those in Fig. 2. The -10 dB bandwidth is almost unaltered. In the following sections of this paper, the width and depth of the EBG structure with the trenches are set to 2.5 mm and 1 mm. The corresponding resonant frequency and -10 dB bandwidth of the EBG structure are 2.54 GHz and 7.9% (2.4 GHz - 2.6 GHz).

B. *Liquids sensor/detector EBG antenna*

The empty trenches (ie. air-filled) may be filled with liquids of different dielectric permittivities, to operate the EBG structure as a wireless sensing system, as shown in Fig. 8(b). A liquid can be characterized by its dielectric constant and loss tangent. To assess its frequency tuning capabilities, the performance of the structure was simulated when the trenches were filled with materials of various dielectric constants and loss tangents, as shown in Fig. 10. Investigations of the influence of these are important for understanding the electromagnetic properties of the overall structure. First, the dielectric permittivities were varied from 1 to 15, and the loss tangent was fixed to 0. The resonant frequency tuned down when the dielectric constant was increased (Fig. 10(a)). For ε_r=1, ε_r=5, ε_r=10 and ε_r=15, the resonant frequency occurred at 2.5 GHz, 2.3 GHz, 2.1 GHz and 1.9 GHz respectively. These compare very well with the studies for the EBG in Fig.3. There was less than 2% deviation from the corresponding resonant frequencies of the unit cell. The -10dB bandwidths were almost unaltered regardless of the changes. In order to assess the effect of dielectric losses, the loss tangent of the trenches was varied from 0 to 0.9, while the dielectric constant was set to 2.

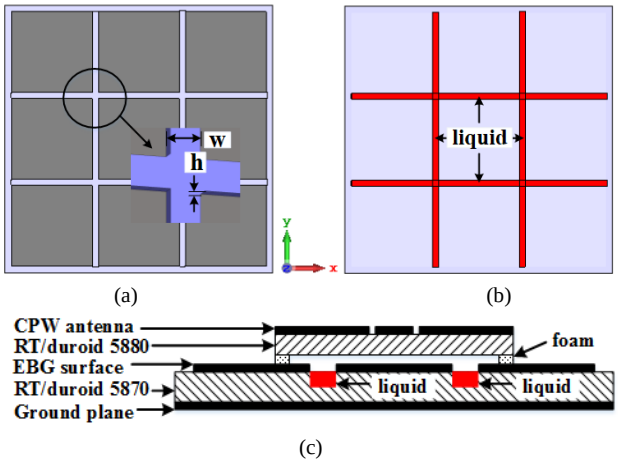

Fig. 8. (a) Top view of the CPW antenna and (b) the EBG structure with trenches (c) Side view of CPW antenna on the EBG substrate with trenches.

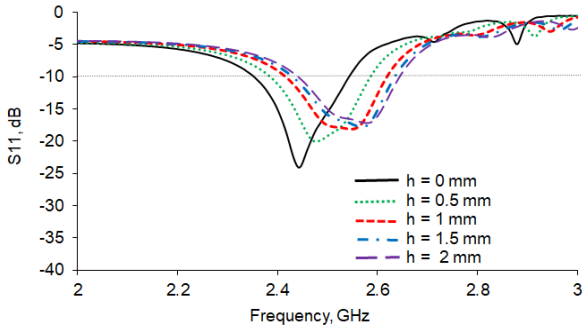

Fig. 9. Simulated reflection coefficient (S_{11}) of the CPW antenna on the EBG structure at different depths (h) of the trenches.

The -10dB bandwidths were wider and the nulls were shallower when the loss tangent was increased (Fig. 10(b)).

Fig. 11(a) shows the sensitivity of the resonance frequency to various trench dielectric constants. This can be expressed by a linear equation of the form:

$$y = 0.0023x + 0.1165 \quad (5)$$

The dependence is almost linear, with an R-squared of 99.6%.

Fig. 11(b) shows the sensitivity to changes in loss tangent from $tan\,\delta$=0 to 0.9 with the fixed $\varepsilon_r = 2$. The resonant frequency was almost unaffected by the various loss tangents.

Four sample liquids giving a range of permittivities were used for the EBG sensor/detector: butan-1-ol, propan-2-ol, ethanol and methanol. Their dielectric properties were chosen from the report [26]. The permittivities of these compounds are very frequency dependent, but at 20^0C at 2.5 GHz they are: $\varepsilon_r = 3.57$ and $tan\,\delta = 0.47$ for Butan-1-ol, $\varepsilon_r = 3.80$ and $tan\,\delta = 0.64$ for Propan-2-ol, $\varepsilon_r = 6.57$ and $tan\,\delta = 0.96$ for ethanol, and $\varepsilon_r = 21.3$ and $tan\,\delta = 0.65$ for methanol. Fig. 12 shows the simulated reflection coefficients when the trenches were filled with the four liquids. In the CST Microwave Studio™, the trenches not filled with any liquid (empty) assume that $\varepsilon_r = 1$ and $tan\,\delta = 0$.

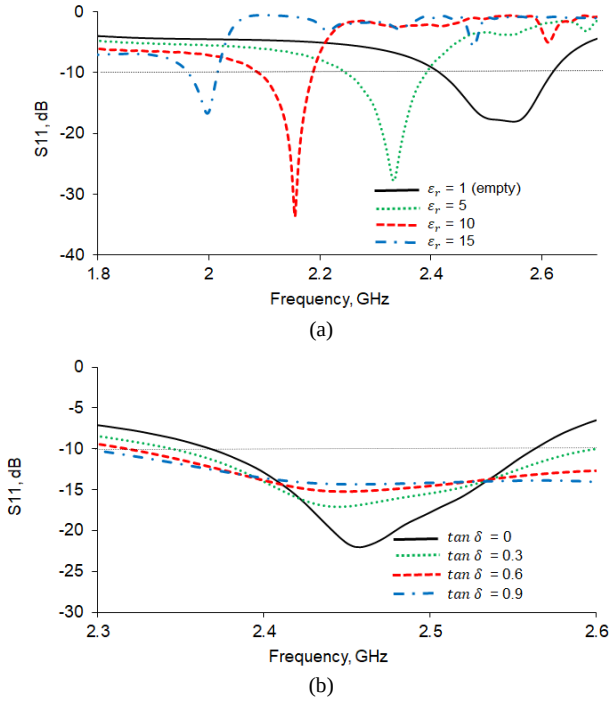

Fig. 10. Simulated dependence of reflection coefficient (S_{11}) of the CPW antenna on (a) dielectric constant (ε_r) and (b) loss tangent ($tan\,\delta$) of the trenches ($\varepsilon_r = 2$).

As shown by the results, the resonant frequency changes according to the different sample liquids. There is a significant effect. As expected, the resonant frequencies with these liquids are lower than that of the empty trench.

The higher loss tangent increases the resonant bandwidth. In particular, methanol has the highest permittivity and provides the greatest frequency shift while ethanol has the highest loss tangent and produces the largest bandwidth. In the case of Butan-1-ol, this complex interaction appears to produce two resonant modes, one at the expected resonant frequency and the other at the frequency of the empty EBG structure.

C. Fabrication and Measurement

To verify the EBG sensor/detector technique based on the sensitivity to liquid permittivity, the structure with trenches was fabricated. Fig. 13 shows a photograph of it. The gaps between the square patches on a substrate were cut out and the depth of trenches adjusted using a 2.5 mm cutter on a high precision milling machine. The trench dimensions were 2.5 mm x 105.4 mm with depth 1mm. The CPW antenna was placed over the EBG structure. The distance between the antenna and the EBG structure with trenches was 5 mm, fixed by rectangular non-conductive polystyrene formers on the edges of antenna substrate using double-sided adhesive tapes.

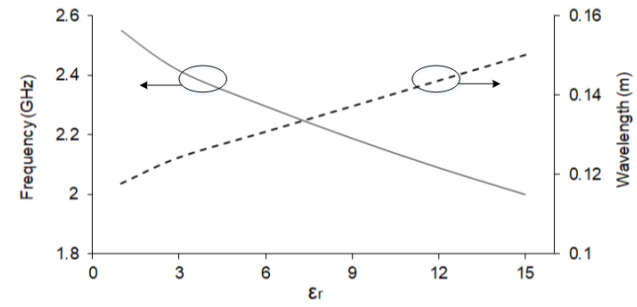

(a)

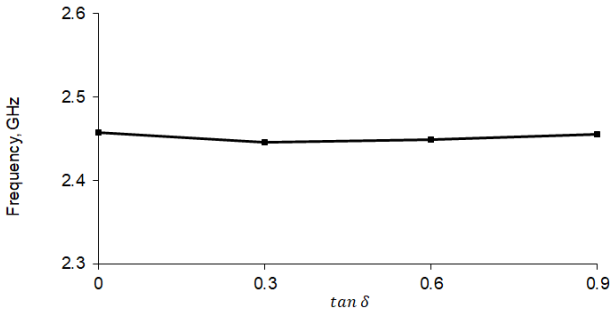

(b)

Fig. 11. Sensitivity of the CPW antenna on the EBG structure: simulated dependence of the resonant frequency and wavelength on (a) trench dielectric constant (b) loss tangent ($tan\ \delta$).

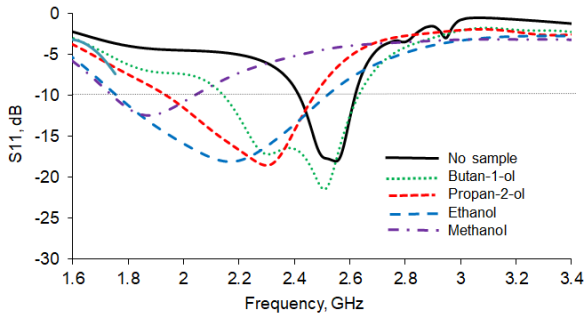

Fig.12. Simulated reflection coefficient (S_{11}) of the antenna with trenches filled with different sample liquids.

The reflection coefficients from the empty trenches were measured and are compared with simulated results in Fig. 14. They are also compared with the results for the CPW antenna on the planar EBG structure. The difference between the simulated and measured results at the resonant frequency is less than 1%. However, the -10 dB measured bandwidth is wider than the simulated ones. The measured reflection coefficient nulls are also deeper than the simulated ones.

The discrepancies may be due to fabrication errors related to accuracy of the trenches made by a milling machine. The trenched EBG structure provides a resonant frequency of 2.53 GHz and a -10 dB bandwidth of 10.3%. The corresponding value of the planar structure is 2.45 GHz and 13.7%.

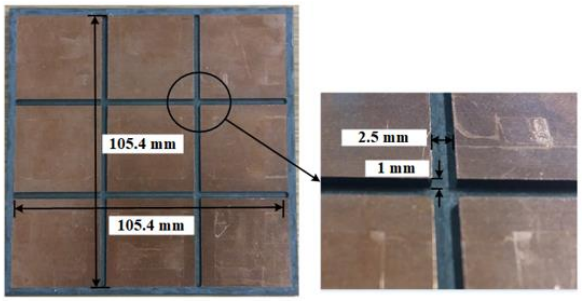

Fig. 13. Photograph of the fabricated EBG structure with empty trenches.

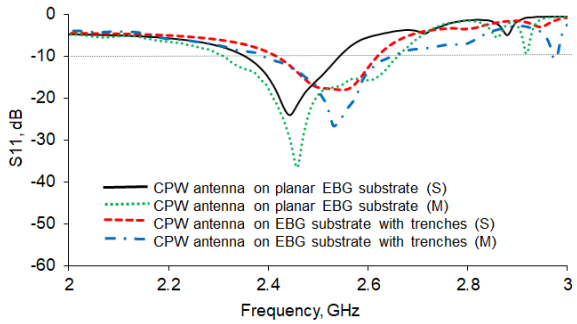

Fig. 14. Reflection coefficient (S_{11}) of the CPW antenna on the EBG substrate with trenches not filled with sample liquids. (S: Simulation, M: Measurement)

For the EBG sensor/detector, preventing liquid leakage from the trench is a significant issue. Fig. 15 shows the fabricated structure. A thin adhesive masking tape (Tesa® 51408 Orange Masking Tape) with thickness of 60µm was used to seal the liquids in the trenches. In the measurement, there was no apparent difference with and without attached adhesive tapes. The four liquids (butan-1-ol, propan-2-ol, ethanol and methanol) were used for the analysis of the EBG array, and each of them has different dielectric constant and loss tangent. They were put into the trenches using a disposable syringe, at room temperature. The radiation patterns were measured in an anechoic chamber. The entire setup was kept at a constant room temperature to ensure constant permittivities.

The input reflection coefficients of the antenna with the four liquids were measured using an Anritsu 37397C vector network analyzer and the results are presented in Fig. 16. It is clear that the various liquids provided a reflection frequency tuning capability for the antenna. The S_{11} profile is noticeably different in term of null depth and bandwidth as well as null frequency allowing different material to be identified. The measured resonant frequencies for butan-1-ol, propan-2-ol, ethanol and methanol were 2.53 GHz, 2.40 GHz, 2.26 GHz, and 2.16 GHz with a reflection coefficient of 21.95 dB, 16.07 dB, 17.70 dB, and 15.24 dB respectively, ie. as might be expected the frequencies decline as ε_r increases.

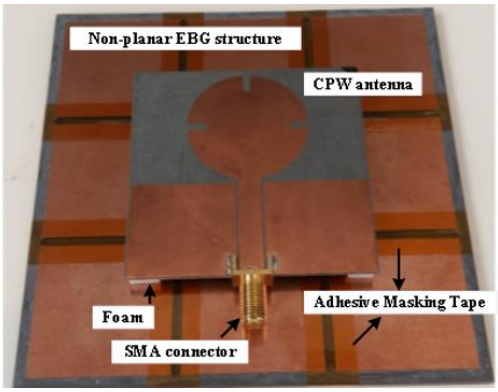

Fig. 15. Photograph of the fabricated antenna on the trenched EBG structure.

It is observed that the measured results differ from the simulated ones (Fig. 12), though follow very similar trend. As aforementioned, there are two resonant modes for butan-1-ol, which coalesce in the measurements to give the impression that the sensor resonates mainly at the same frequency as the empty structure. The differences may be due to errors in the fabrication process, potential differences in the dielectric permittivities and loss tangent from those stated in [26], and deviations in the quantity, quality and temperature of the liquids in the trenches compared with ideal simulated cases.

For the sake of completion, Fig. 17 presents measured normalized antenna radiation patterns for two liquids (propan-2-ol, and ethanol). It is observed that EBG structure improves the directivity in all cases. There are measured losses as the liquids are lossy (section III. B). The simulated gain of the empty (unfilled), propan-2-ol, and ethanol examples were 9 dB, 1.2 dB and 1.0 dB at 2.53 GHz, 2.40 GHz, and 2.26 GHz respectively. The measured gain was about the same for the empty case and -3.7 dB and -3.0 dB for the two liquids tested.

IV. Discussion and Conclusion

A novel reconfigurable EBG technique suitable for sensing applications has been demonstrated. The reconfigurable behavior of the EBG is obtained by creating trenches between the unit cells and filling them up with liquids of different permittivities. The changes in permittivity produce a change in the resonant frequency of the EBG structure. This EBG sensor could be used as standalone solution where the reflected signal can be evaluated. An alternative solution is to use an antenna in close proximity to the EBG structures. The latter was investigated in the paper. A CPW antenna was designed and located at the center of the EBG structure, with the trenches filled with the four different sample liquids: butan-1-ol, propan-2-ol, ethanol and methanol. The EBG structure reduces the bandwidth of the CPW antenna and therefore increases its potential as a sensor. This first concept of such a sensor has shown good sensitivity and linear response for lossless materials. The technique is applicable to reconfigurable antennas, with liquids such as the paraffins [19]. When liquids with higher loss tangent are tested, the sensitivity is reduced. A potential solution is the use of a different type of EBG element such as the narrowband convoluted EBG designs [27].

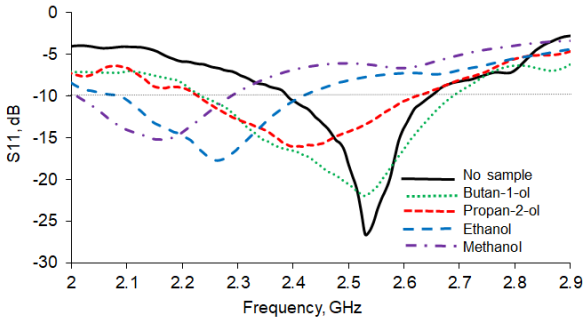

Fig.16. Measured reflection coefficient (S_{11}) of the CPW antenna on the EBG substrate with trenches filled with liquids.

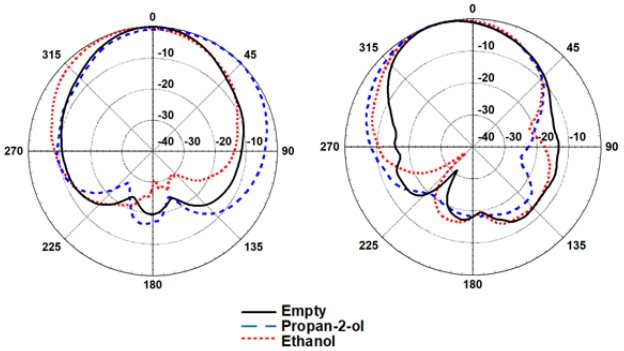

(a) (b)

Fig.17. Measured radiation patterns of the CPW antenna on the EBG structure with trenches filled with empty, propan-2-ol, and ethanol at 2.53 GHz, 2.40 GHz, and 2.26 GHz (a) *xz* plane (b) *yz* plane.

The sensor/detector technique can be integrated as part of a wireless sensor network. A possible use is illustrated in Fig.18. In this case, the sensor is placed in a flooring or drainage system where liquids may fall by precipitation and may be guided towards the EBG sensor. These liquids will fall into the trenches, which will be filled. The filling will lead to a change in the resonant frequency of the EBG. This change could be picked up through the change of S_{11} of the antenna described in this paper. Alternatively, the EBG by itself (without the antenna) could work as a reflector and an external signal could be sent and compared with the reflected one. This is something that could be explored in the future.

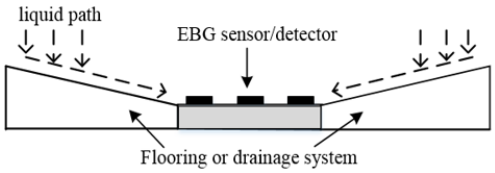

Fig.18. Arrangement of the potential EBG sensor/detector.

References

[1] D. Sievenpiper, L. Zhang, R. F. Broas, N. G. Alexopolous, and E. Yablonovitch, "High-impedance electromagnetic surfaces with a forbidden frequency band", *IEEE Trans. Microw. Theory Tech.*., vol. 47, no. 11, pp. 2059–2074, Nov. 1999.

[2] D. Sievenpiper, J. Colburn, B. Fong, J. Ottusch, J. Visher, ″Holographic artificial impedance surfaces for conformal antennas,” in *IEEE Int. Symp. Dig. Antennas Propag.*, Jul. 2005, pp. 256–259.
[3] A. P. Feresidis, G. Goussetis, S. Wang, and J. C. Vardaxoglou, "Artificial magnetic conductor surfaces and their application to low-profile high gain planar antennas", *IEEE Trans. Antennas Propag.*, vol. 53, no. 1, pp. 209–215, Jan. 2005.
[4] S. Zhu and R. Langley, "Dual-Band Wearable Textile Antenna on an EBG Substrate", *IEEE Trans. Antennas Propag.*, vol. 57, pp. 926-935, Apr. 2009.
[5] H. R. Raad, A. I. Abbosh, H. M. Al-Rizzo, and D. G. Rucker, "Flexible and Compact AMC Based Antenna for Telemedicine Applications", *IEEE Trans. Antennas Propag.*, vol. 61, pp. 524-531, Feb. 2013.
[6] X. L. Bao, G. Ruvio, M. J. Ammann, and M. John, "A novel GPS patch antenna on a fractal hi-impedance surface substrate", *IEEE Antennas Wireless Propag. Lett.*, vol. 5, no. 1, pp. 323–326, Dec. 2006.
[7] B. Gao, C. H. Chen, and M. M. F. Yuen, "Low-cost passive UHF RFID packaging with electromagnetic band gap (EBG) substrate for metal objects", in *Proc. Electronic Components and Technology Conf. ECTC'07*, 2007, pp. 974–978.
[8] M. J. Al-Hasan, T. A. Denidni, and A. R. Sebak, "Millimeter-Wave EBG-Based Aperture-Coupled Dielectric Resonator Antenna", *IEEE Trans. Antennas Propag.*, vol. 61, pp. 4354-4357, Aug. 2013.
[9] M.J. Al Hasan, T.A Denidni and A. R. Sebak, “Millimeter-wave EBG antenna pattern diversity”, in *IEEE Int. Symp. Dig. Antennas Propag.*, Jul. 2013, pp 272-273.
[10] H. J. Lee, K. L. Ford, and R. J. Langley, "Dual band tunable EBG", *Electron. Lett.*, vol. 44, no. 6, pp. 392–393, Mar. 2008.
[11] B. Schoenlinner, A. Abbaspour-Tamijani, L. C. Kempel, and G. M. Rebeiz, "Switchable low-loss RF MEMS Ka-band frequency-selective surface", *IEEE Trans. Microw. Theory Tech.*, vol. 52, pp. 2474-2481, Nov. 2004.
[12] F. Yang and Y. Rahmat-Samii, "Polarization-dependent electromagnetic bandgap surfaces: Characterization, designs, and applications", in *IEEE Int. Symp. Dig. Antennas Propag.*, Jun. 2003, pp. 339–342.
[13] W. Yang, W. Che, H. Jin, W. Feng, and Q. Xue, "A Polarization-Reconfigurable Dipole Antenna Using Polarization Rotation AMC Structure", *IEEE Trans. Antennas Propag.*, vol. 63, pp. 5305-5315, Dec. 2015.
[14] B. Liang, B. Sanz-Izquierdo, E. A. Parker, and J. C. Batchelor, "A Frequency and Polarization Reconfigurable Circularly Polarized Antenna Using Active EBG Structure for Satellite Navigation", *IEEE Trans. Antennas Propag.*, vol. 63, pp. 33-40, Jan. 2015.
[15] D. Sievenpiper, J. Schaffner, J. J. Lee, and S. Livingston, "A steerable leaky-wave antenna using a tunable impedance ground plane", *IEEE Antennas Wireless Propag. Lett.*, vol. 1, pp. 179-182, Oct. 2002.
[16] J. W. Sanders, J. Yao, and H. Huang, “Microstrip patch antenna temperature sensor”, *IEEE Sensors J.*, vol. 15, no. 9, pp. 5312–5319, Sep. 2015.
[17] F. Yang, Q. Qiao, J. Virtanen, A. Z. Elsherbeni, L. Ukkonen, and L. Sydänheimo, “Reconfigurable sensing antenna: A slotted patch design with temperature sensation”, *IEEE Antennas Wireless Propag. Lett.*, vol. 11, pp. 632–635, Jun. 2012.
[18] H. Lobato-Morales, A. Corona-Chávez, J. L. Olvera-Cervantes, R. A. Chávez-Pérez, and L. José, "Wireless Sensing of Complex Dielectric Permittivity of Liquids Based on the RFID", *IEEE Trans. Microw. Theory Tech.*, vol. 62, pp. 2160-2167, Sep. 2014.
[19] A. C. de C. Lima, E. A. Parker, and R. J. Langley, "Tunable frequency selective surface using liquid substrates", *Electron Lett.*, vol. 30, pp. 281-282, Feb. 1994.
[20] M. Labidi, J. B. Tahar, and F. Choubani, “Meta-materials applications in thin- film sensing and sensing liquids properties”, *Opt. Exp.*, vol. 19, no. S4, pp. A733–A739, May 2011.
[21] A. Ebrahimi, W. Withayachumnankul, S. Al-Sarawi, and D. Abbott, “High-sensitivity metamaterial-inspired sensor for microfluidic dielectric characterization”, *IEEE Sensors J.*, vol. 14, no. 5, pp. 1345–1351, May 2014.
[22] A. Sadeqi, H. R. Nejad, and S. Sonkusale, "Low-cost metamaterial-on-paper chemical sensor", *Opt. Exp.*, vol. 25, pp. 16092-16100, Jul. 2017.
[23] R. Yadav and P. N. Patel, “Experimental study of adulteration detection in fish oil using novel PDMS cavity bonded EBG inspired patch sensor”, *IEEE Sensors J.*, vol. 16, no. 11, pp. 4354–4361, Jun. 2016.
[24] S. B. Yeap and Z. N. Chen, "Microstrip Patch Antennas With Enhanced Gain by Partial Substrate Removal", *IEEE Trans. Antennas Propag.*, vol. 58, pp. 2811-2816, Sep. 2010.
[25] J. Liang, L. Guo, C. C. Chiau, X. Chen, and C. G. Parini, "Study of CPW-fed circular disc monopole antenna for ultra wideband applications", *IEE Proc. Microw. Antennas Propag.*, vol. 152, pp. 520-526, Dec. 2005.
[26] A. P. Gregory and R. N. Clarke, “Tables of the complex permittivity of dielectric reference liquids up to 5 GHz”, *CETM*, Teddington, U.K., Nat. Phys. Rep. 33, Jan. 2012.
[27] S. Tse, B. Sanz Izquierdo, J.C. Batchelor and R.J. Langley, "Convoluted elements for electromagnetic band gap structures", in *IEEE Int. Symp. Dig. Antennas Propag.*, Jun. 2004, pp. 819-822.